



Polymer Communication

Improved fracture toughness of immiscible polypropylene/ethylene-co-vinyl acetate blends with multiwalled carbon nanotubes

Li Liu, Yong Wang*, Yanli Li, Jun Wu, Zuowan Zhou, Chongxi Jiang

Key Laboratory of Advanced Technologies of Materials (Ministry of Education), School of Materials Science and Engineering, Southwest Jiaotong University, Erhuan Road, North 1, No. 111, Chengdu, Sichuan 610031, China

ARTICLE INFO

Article history:

Received 16 December 2008
 Received in revised form
 24 April 2009
 Accepted 29 April 2009
 Available online 8 May 2009

Keywords:

PP/EVA
 Fracture toughness
 Multiwalled carbon nanotubes

ABSTRACT

Functionalized multiwalled carbon nanotubes (f-MWCNTs) have been introduced into immiscible polypropylene/ethylene-co-vinyl acetate (PP/EVA) blends. Two different compositions, one (PP/EVA = 80/20) exhibits the typical sea-island morphology and the other (PP/EVA = 60/40) exhibits the cocontinuous morphology, have been prepared with different contents of f-MWCNTs. The impact measurement shows that f-MWCNTs induce the great improvement of fracture toughness of cocontinuous PP/EVA blends. The results based on the morphologies and the rheological properties of the composites suggest that, a local “single-network structure” of f-MWCNTs exists in PP/EVA (80/20) system whereas a “dual-network structure” of f-MWCNTs and EVA phase exists in PP/EVA (60/40) system, and the latter structure accounts for the largely improved fracture toughness of the composites.

© 2009 Elsevier Ltd. All rights reserved.

1. Introduction

Recently, some researches have been carried out to investigate the fracture toughness of polymer with carbon nanotubes (CNTs). It has been reported that the orientation of CNTs as well as their good dispersion is an efficient way to substantially toughen the composites [1–3]. Some toughening mechanisms, including the bridge effect of the oriented CNTs on the craze and crack development during the applied stress in the tensile test [1,2,4], the enhanced load-carrying ability and the much-increased deformability of nanotubes-filled composites [5–7], have been proposed based on the analysis of the fractured surface morphologies of composites.

Besides the application of CNTs in single polymer matrix, other researches have shown that CNTs also exhibit apparent roles in influencing the morphologies, mechanical and electrical properties of polymer blends. Khare et al. [8] revealed a refinement in the morphology whether particle dispersed type or cocontinuous structure in the presence of CNTs in polypropylene/acrylonitrile-butadiene-styrene (PP/ABS) blends, and lower electrical percolation threshold was observed in continuous PP/ABS blends with CNTs. Li Y [9] reported that the addition of CNTs into polyamide-6 (PA6) significantly increases the melt viscosity of PA6, and a phase transformation from sea-island to cocontinuous occurs upon adding more than 1.2 wt% CNTs into the blends. Both the electrical conductivity

and the ductility of the obtained composites were greatly improved. Among all these researches, the formation of the dual percolation was believed to be the main reason accounting for the improvement of the electrical properties of polymer blends [8,9].

In this work, our attention is paid to the improvement of fracture toughness of immiscible polymer blends such as polypropylene/ethylene-co-vinyl acetate (PP/EVA). PP/EVA blends have been widely investigated due to their poor interfacial bonding. With the increasing content of EVA in PP, the blend morphology changes from sea-island to cocontinuous morphology [10]. Thus, PP/EVA blends with two typical morphologies, i.e. sea-island (PP/EVA = 80/20) and cocontinuous (PP/EVA = 60/40) morphologies, according to the reported references, are selected in the research. f-MWCNTs are introduced into the phase of EVA through a controlled melt-blending sequence, namely, f-MWCNTs are firstly dispersed in EVA phase. The blend sequence is set based on the fact that CNTs tend to migrate to the PP phase owing to their good affinity for polyolefin during melt-blending [11]. It is expected that CNTs could form the network structure in the whole system, strengthening the interfacial bonding between the phases of EVA and PP, and finally leading to the great change in fracture toughness of such immiscible polymer blends.

2. Experimental

2.1. Materials

All the materials used in this study are commercially available. PP (F401, Lanzhou Petrochemical Co, Ltd., Lanzhou, China) with

* Corresponding author. Tel.: +86 28 87602714; fax: +86 28 87600454.
 E-mail address: yongwang1976@163.com (Y. Wang).

a melt flow rate (MFR) of 2.5 g/10 min (230 °C/2.16 kg) was used as the matrix polymer. EVA (ELVAX460, 18% VA, DuPont Industrial Polymers, USA) with an MFR of 2.5 g/10 min was selected as impact modifier. MWCNTs were obtained from Chengdu Institute of Organic Chemistry, Chinese Academy of Science (Chengdu, China). The outer and inner diameters of MWCNTs are 20–30 nm and 5–10 nm, respectively. The length of a single MWCNT is about 10–50 μm . MWCNTs were washed and purified with concentrated hydrochloric acid, and the purity is more than 95% in weight base.

2.2. Sample preparation

To achieve a good dispersion, pristine MWCNTs must be chemically modified prior to blend with polymers. The functionalization of MWCNTs was carried out according to Ref. [12]. The pristine MWCNTs were mixed with concentrated HNO_3 to obtain the acid-MWCNTs with carboxyl and hydroxyl groups on the outer surface of MWCNTs. Then the acid-MWCNTs were reacted with maleic anhydride in the solution of concentrated HCl and ethyl acetate at 60 °C for 5 h under sonication to obtain the maleic anhydride functionalized MWCNTs (f-MWCNTs). After functionalization, more functional groups including carboxyl, hydroxyl and carbonyl were introduced into MWCNTs. These functional groups are favorable to the formation of hydrogen bonding between f-MWCNTs and VA chain segments, resulting in good dispersion of f-MWCNTs in EVA phase. In this work, the master batch of EVA with 10 wt% f-MWCNTs was prepared firstly. Then, the master batch was blended with different contents of PP and EVA to obtain the corresponding compositions. In this work, the contents of EVA and f-MWCNTs were set as 20, 40 wt% and 0, 0.5, 1.0, 2.0 wt% of the blend, respectively. The blending of such samples was carried out on a twin-screw extruder (TSSJ-25, China) at the screw speed of 110 r/min and the temperatures of 140–200 °C from hopper to die. After making droplets, the pellets were injection molded through an injection-molding machine (KTEC-40, Germany) at the melt temperatures of 190–210 °C and mould temperature of 25 °C. Furthermore, EVA nanocomposites with only f-MWCNTs were melting blended through using a Lab-station Brabender torque rheometer (Plasti-Corder, Germany) with the setting temperature of 140 °C. The melt-blending time was 8 min and the rotor speed was 60 rpm.

2.3. Impact test

Notched Izod impact strength was measured using an XC-22Z impact tester (China) according to ISO180-2000. For each blend, the average value reported was derived from at least five specimens. The testing was carried out at room temperature (23 °C).

2.4. Characterizations

The morphologies of EVA in the blends were characterized by using a Fei Quanta 200 SEM (USA) with an accelerating voltage of 20 kV. Sample was cryogenically fractured perpendicular to flow direction after being immersed in liquid nitrogen for 0.5 h, then the sample was etched in toluene at 50 °C for 3 h to remove EVA phase from PP matrix. To investigate the dispersion of f-MWCNTs in the blends, the cryogenically fractured surface was firstly ion-etched at 15 kV for 10 min through NP-IX-ray Photoelectron Spectroscopy (China), and then the ion-etched surface was characterized by SEM too.

The rheological measurement was carried out on a stress controlled rheometer (rheometer System Gemini 200, Germany) using a 20 mm diameter parallel plate. The sample disk was firstly prepared with a thickness of 1.0 mm and a diameter of 20 mm

through a compression molding way at 200 °C for 5 min. During the rheological measurement process, the frequency sweep from 0.01 to 100 rad/s was performed at 190 °C under dry nitrogen atmosphere. For all the measurements, the samples were tested within the linear viscoelastic strain range.

3. Results and discussion

3.1. Impact strength

Generally, the immiscible polymer blends show poor mechanical properties because of the weak interface between the two phases. Although EVA has been proved to improve the fracture toughness of PP [13], the toughening effect is still inconspicuous. As shown in Fig. 1, even if the content of EVA is up to 40 wt%, the impact strength is only 10.2 kJ/m^2 , more inferior to the fracture toughness of ethylene–octene copolymer toughened PP blends [14]. The addition of a few amount of f-MWCNTs induces the change of fracture toughness of composites in different degrees, and the improvement of impact strength is greatly dependent of the contents of EVA and f-MWCNTs. For PP/EVA (80/20) system, the impact strength increases slightly with the increasing content of f-MWCNTs, indicating that f-MWCNTs don't influence the fracture toughness of such blend significantly. However, for PP/EVA (60/40) system, the impact strength increases greatly with increasing content of f-MWCNTs. For example, addition of 2 wt% f-MWCNTs induces the enhancement of impact strength from 10.2 kJ/m^2 of PP/EVA (60/40) to 63.2 kJ/m^2 of PP/EVA/f-MWCNTs (60/40/2), about 6 times of impact strength improvement is observed. Considering the impact strength of pure PP (4.2 kJ/m^2 , not shown in the graph), one also can see that EVA and f-MWCNTs exhibit synergistic toughening effect for PP when more EVA is present in the composites, for example, 40 wt%. Importantly, for immiscible PP/EVA blends with high content of EVA, the addition of f-MWCNTs induces the great enhancement of impact strength. This may provide a simple but efficient way to improve the mechanical properties of such immiscible polyolefin blends.

3.2. Morphologies

Before the characterization of the phase morphology and the distribution of f-MWCNTs in PP/EVA blends, some schematic representations of composites are proposed and shown in Fig. 2. For

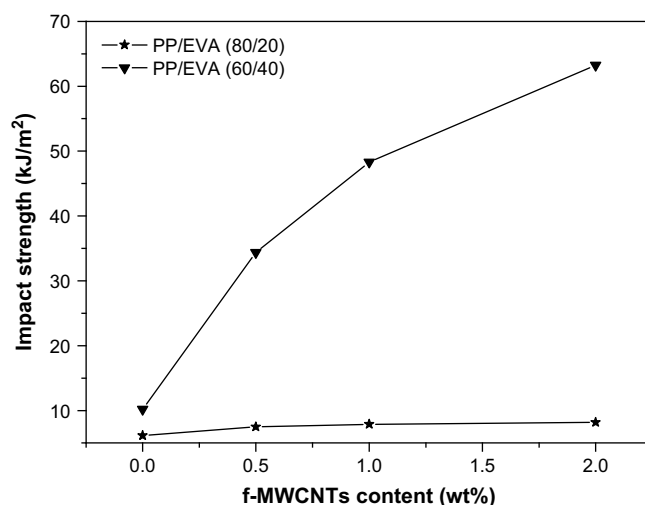


Fig. 1. Notched Izod impact strength of PP/EVA blends with different contents of f-MWCNTs.

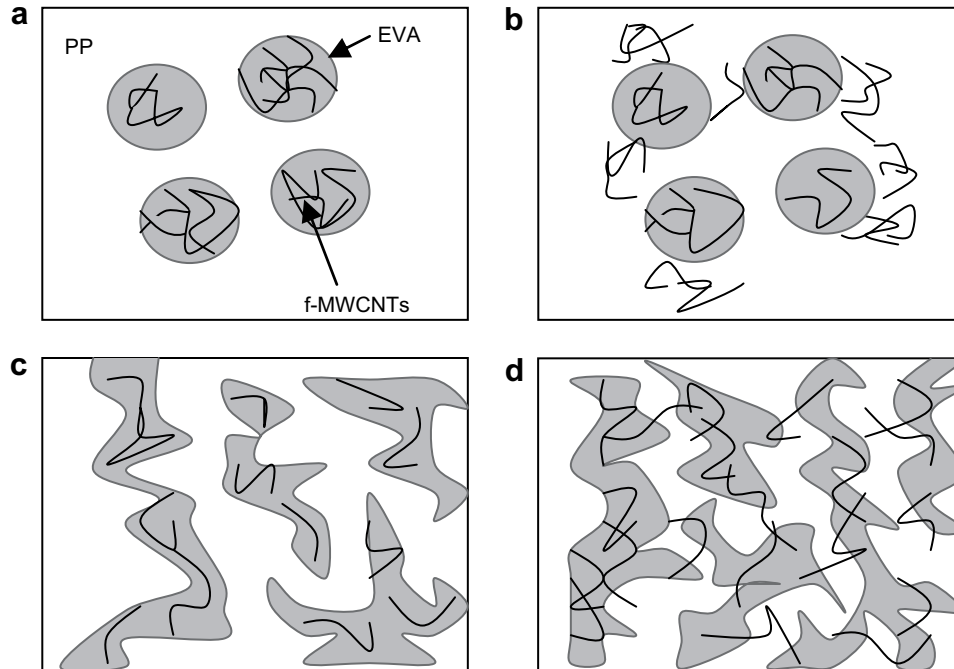


Fig. 2. Schematic representations show the dispersion states of f-MWCNTs in PP/EVA blends. (a): f-MWCNTs tend to aggregate in dispersed EVA phase in PP/EVA (80/20) at low load; (b): f-MWCNTs migrate to PP phase and form a local “single-network structure” at high load; (c): f-MWCNTs exhibit good dispersion in continuous phase of EVA in PP/EVA (60/40) at low load and (d): f-MWCNTs form the network structure in the whole blend.

PP/EVA (80/20) system with low f-MWCNTs content, f-MWCNTs tend to form the clusters, which are limited in the EVA phase (Fig. 2a); at high f-MWCNTs content, these clusters migrate to PP phase, possibly inducing the local network structure or aggregation of f-MWCNTs around EVA particles (Fig. 2b). For PP/EVA (60/40) system, f-MWCNTs exhibit good dispersion in EVA phase at low load due to the largely increased EVA phase and the good interaction between EVA and f-MWCNTs (Fig. 2c). At high load, f-MWCNTs form the network structure in EVA phase. Furthermore, some f-MWCNTs tend to migrate to PP phase, possibly inducing some f-MWCNTs span the two phases, leading to the bridge effect for PP and EVA (Fig. 2d). In PP/EVA (80/20) system, only f-MWCNTs can form the local network structure in PP phase (named as “single-network structure”), whereas EVA presents as the isolated particles. In PP/EVA (60/40) system, besides the network structure of f-MWCNTs, PP and EVA exhibit a certain degree of interpenetration

effect and in this condition, one can hypothesize that EVA also form the continuous “network structure”. Thus, a so called “dual-network structure” of f-MWCNTs and EVA forms in this system. Here, the concept of “dual-network structure” is very similar to the “double percolation” concept first introduced by Sumita [15] in investigating the electrical properties of conductive materials.

Figs. 3–6 show the morphologies of PP/EVA/f-MWCNTs composites as well as the dispersion states of f-MWCNTs in the composites characterized through SEM. Because f-MWCNTs are firstly controlled to disperse in EVA phase and the dispersion states of f-MWCNTs in the composites are difficult to be characterized by usual chemical etching due to the fact that most of f-MWCNTs can be dissolved together with EVA phase, thus the ion etching combined with SEM was selected to characterize the dispersion of f-MWCNTs. As shown in Fig. 3, for PP/EVA/f-MWCNTs (80/20/2) composite, f-MWCNTs tend to aggregate together and form the

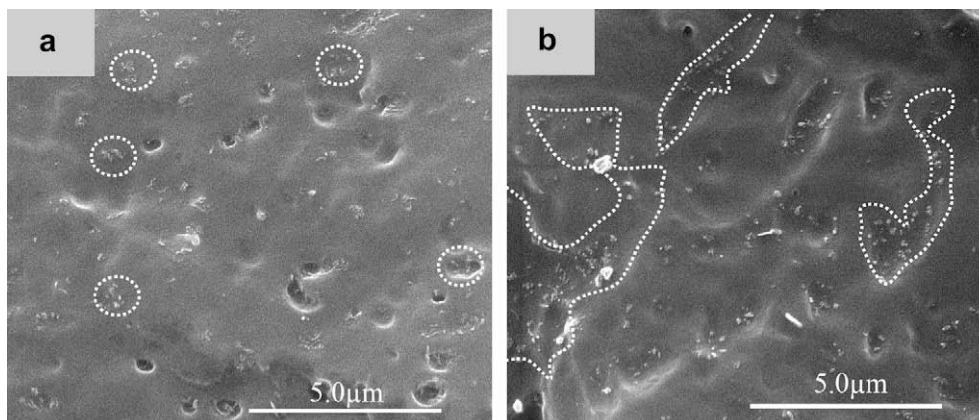


Fig. 3. SEM image shows the dispersion of f-MWCNTs in (a) PP/EVA/f-MWCNTs (80/20/2) and (b) PP/EVA/f-MWCNTs (60/40/2) composites. Samples were ion-etched prior to SEM measurement.

dispersed clusters in the system (as shown in the white circle in Fig. 3(a)). For PP/EVA/f-MWCNTs (60/40/2) composite, f-MWCNTs exhibit good dispersion in the composite. If we draw a graph to contain the local area which f-MWCNTs are present, one can notice that f-MWCNTs tend to form the “continuous morphology”. This can be ascribed to the fact that most of f-MWCNTs are dispersed in the continuous phase of EVA (as shown in Fig. 3(b)).

In Figs. 4 and 5, EVA phase was chemically etched by toluene. For PP/EVA (80/20) blend, as shown in other research [10], the blend exhibits the typical sea-island morphology (Fig. 3(a)). At low f-MWCNTs concentrations (0.5 and 1 wt%), f-MWCNTs tend to maintain in the EVA phase and very few f-MWCNTs can be observed in the matrix or in the interface (Fig. 4(b) and (c)). This result is consistent with the previous hypothesis that f-MWCNTs are mainly distributed in the EVA phase. When EVA phase is dissolved during the chemical treatment, f-MWCNTs are also dissolved too. However, once the content of f-MWCNTs is increased up to 2.0 wt%, a lot of f-MWCNTs are observed in the matrix (Fig. 4(d)), indicating the migration of f-MWCNTs from EVA phase to PP phase during the blending process. In this work, although MWCNTs were functionalized by maleic anhydride, which strengthens the interaction between f-MWCNTs and EVA through the hydrogen bonding, the average diameter of EVA particles is about 1–1.5 μm , much smaller than the length of f-MWCNTs. In this condition, f-MWCNTs at high load tend to self-entangle and form the clusters with large size, exceeding the diameter of EVA particles and resulting some clusters of f-MWCNTs migrate to the PP phase, possibly form the local network structure of f-MWCNTs around EVA particles (the so called “single-network structure” shown in Fig. 2(b)).

Fig. 5 shows the morphologies of PP/EVA (60/40) blend with different contents of f-MWCNTs. The typical cocontinuous morphologies are observed for all the compositions. The presence of f-MWCNTs doesn't change such morphologies apparently. However, one can observe that f-MWCNTs bridge EVA phase and PP phase at higher concentrations, such as 1.0 and 2.0 wt% (Fig. 5(c) and (d)). This can be ascribed to the fact that the length of a single nanotube is longer than the particle or the ligament size of EVA, during the melt-blending process, the migration of nanotubes from EVA phase to PP phase may induce one nanotube span the two phases, leading to the bridge effect for PP and EVA. The chain segments of f-MWCNTs with functional groups (maleic anhydride) maintain in EVA phase through the hydrogen bonding effect between carboxyl groups and VA chain segments, and the other chain segments of f-MWCNTs without functional groups migrate to PP phase. Through the bridge effect of f-MWCNTs, the interfacial bonding of immiscible PP/EVA blend is greatly strengthened. Fig. 6 shows the distribution of f-MWCNTs at higher magnifications. Besides the bridge effect of f-MWCNTs in the interface, one also can see that f-MWCNTs tend to form the network structure in the EVA phase (as shown in the white circle), and the so called “dual-network structure” is observed, which may be the main reason for the largely improved impact toughness of PP/EVA/f-MWCNTs (60/40/1 and 60/40/2) composites.

3.3. Rheological properties

Fig. 7 shows the variation of storage modulus (G') and melt viscosity (η^*) with frequency for various compositions at 190 $^{\circ}\text{C}$. For PP/EVA (80/20) system, the addition of only 1.0 wt% f-MWCNTs induces the great enhancement of G' and η^* . Further increasing

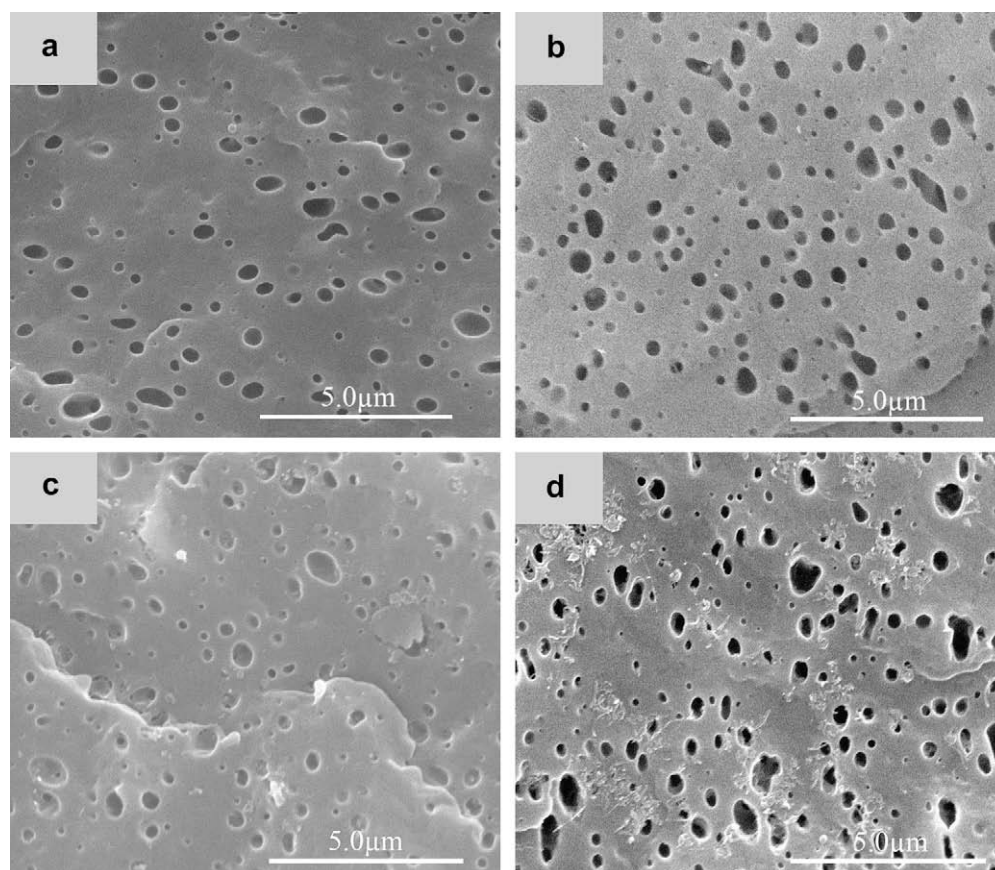


Fig. 4. SEM images of PP/EVA (80/20) with different contents of f-MWCNTs. (a) 0 wt%, (b) 0.5 wt%, (c) 1 wt%, (d) 2 wt%.

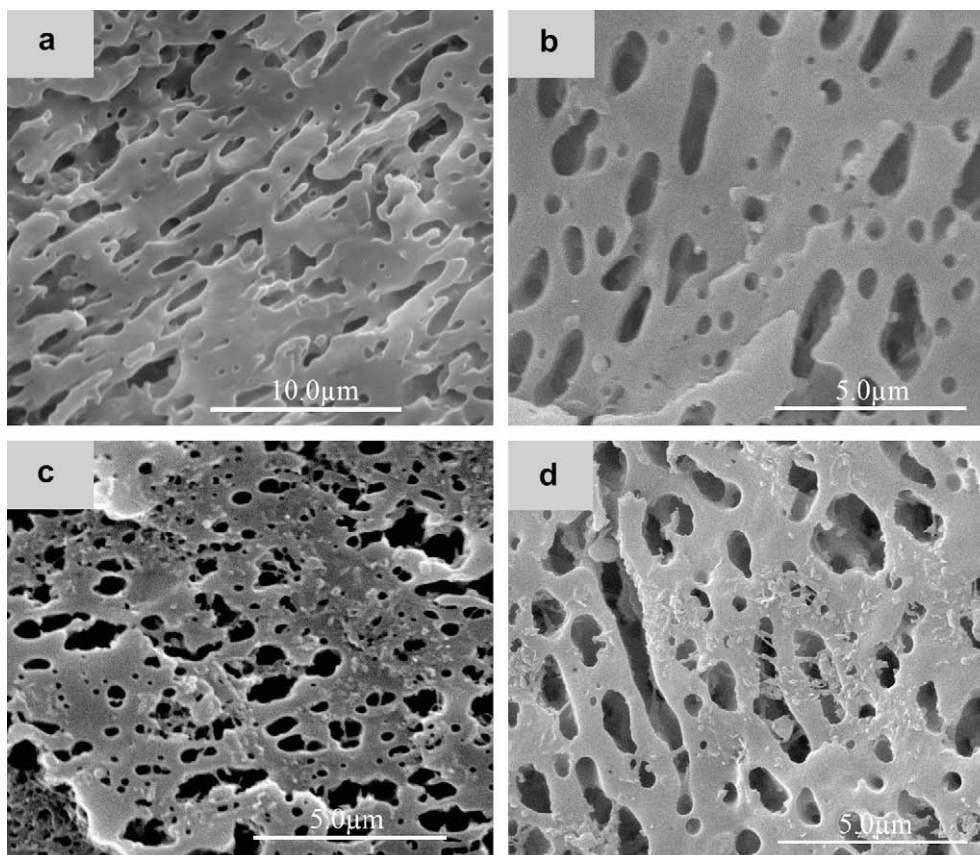


Fig. 5. SEM images of PP/EVA (60/40) with different contents of f-MWCNTs. (a) 0 wt%, (b) 0.5 wt%, (c) 1 wt%, (d) 2 wt%.

f-MWCNTs induces the further enhancement of G' and η^* slightly. This is most likely ascribed to the migration of f-MWCNTs from EVA phase to PP phase at high f-MWCNTs load and in this condition, the effect of f-MWCNTs on G' and η^* is available. However, for PP/EVA (60/40) system, the addition of f-MWCNTs exhibits weak effect on the G' and η^* possibly due to the largely increased EVA phase compared to PP/EVA (80/20). Although it is expected that the change of G' would prove the presence of network structure of f-MWCNTs in PP/EVA/f-MWCNTs composites through the development of a plateau at low frequency [8], no evidence can prove the

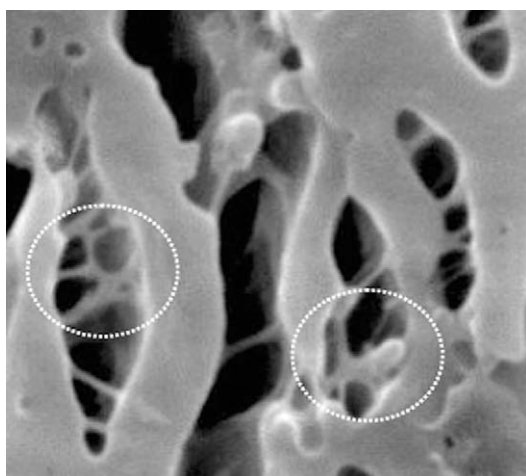


Fig. 6. SEM image shows the morphology of PP/EVA/f-MWCNTs (60/40/2) at higher magnification.

formation of f-MWCNTs network structure in the composites most likely due to the fact that the melt temperature of 190 °C is much higher than that of the fusion temperature (T_m) of EVA (the fusion temperature of EVA used in the work is about 87 °C), and the rheological properties of the composites are mainly controlled by EVA rather than by f-MWCNTs.

Thus, the rheological properties of EVA with f-MWCNTs were measured to prove the presence of the network structure of f-MWCNTs in PP/EVA (60/40) ternary composites indirectly. In order to make a comparison between PP/EVA/f-MWCNTs ternary composites and EVA/f-MWCNTs binary composites, it is very important to maintain the consistent of the f-MWCNTs content. Thus, EVA composites with 1.25, 2.5 and 5 wt% f-MWCNTs were prepared. During the rheological measurement, the melt temperature was set as 150 °C. As shown in Fig. 8, G' and η^* increase with increasing f-MWCNTs. Once the content of f-MWCNTs is up to 2.5 wt%, the composite exhibits a visible plateau in storage modulus, and the plateau becomes more apparent at 5 wt% f-MWCNTs, indicating the formation of the network structure of f-MWCNTs. Combining the results obtained from SEM (Figs. 4 and 5), one can believe that the network structure of f-MWCNTs develops easily in the cocontinuous PP/EVA (60/40) blends.

3.4. Toughening mechanism

The above results show that only local “single-network structure” of f-MWCNTs forms in PP/EVA (80/20) system, whereas “dual-network structure” of f-MWCNTs and EVA forms in PP/EVA (60/40) system. It is clear that the morphological difference between the two systems accounts for the improvement of fracture

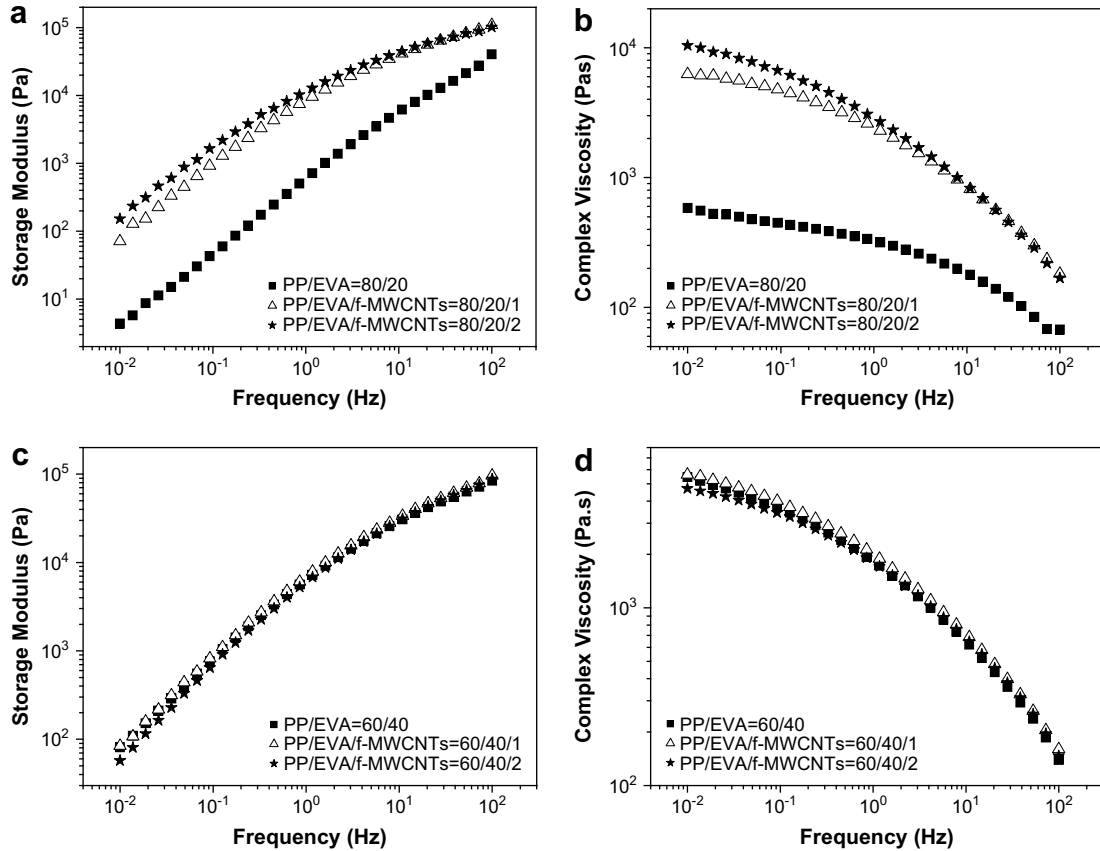


Fig. 7. Rheological properties of PP/EVA (80/20) and (60/40) melts containing different contents of f-MWCNTs: (a) and (c) storage modulus (G'), (b) and (d) complex viscosity (η^*).

toughness in different degrees when f-MWCNTs are introduced into them. In the former system, although f-MWCNTs have a high affinity with PP, they mainly locate in EVA phase at low load and in this condition, f-MWCNTs tend to aggregate together due to the length of a single carbon nanotube range from 10 to 50 μm , which is much longer than the diameter of EVA particles; at high load, the clusters of f-MWCNTs migrate from EVA phase to around PP phase, resulting the local network structure or aggregation. Thus the network structure of f-MWCNTs in PP/EVA (80/20) is very poor, and the interfacial bonding between PP and EVA is very weak too. The similar network structure of filler has been reported in polypropylene/ethylene-propylene-diene terpolymer/silicon dioxide (PP/EPDM/SiO₂) composites, in which nano-SiO₂ forms the

network structure around EPDM phase, and such network structure is thought to be the main reason for the great improvement of impact toughness of composites [16,17]. However, in this work, the network structure of f-MWCNTs in PP/EVA (80/20) is very poor. Contrarily, the local aggregation of f-MWCNTs in PP phase most likely induces the severe stress concentration, which is unfavorable to the improvement of fracture toughness.

In the latter system, EVA exhibits the continuous morphology, which is in favor of the exfoliation and well dispersion of f-MWCNTs in EVA phase. Furthermore, it is evident that the cocontinuous morphology has much more interfacial area with respect to the sea-island morphology, making more chances for f-MWCNTs to migrate into PP phase or span the two phases due to

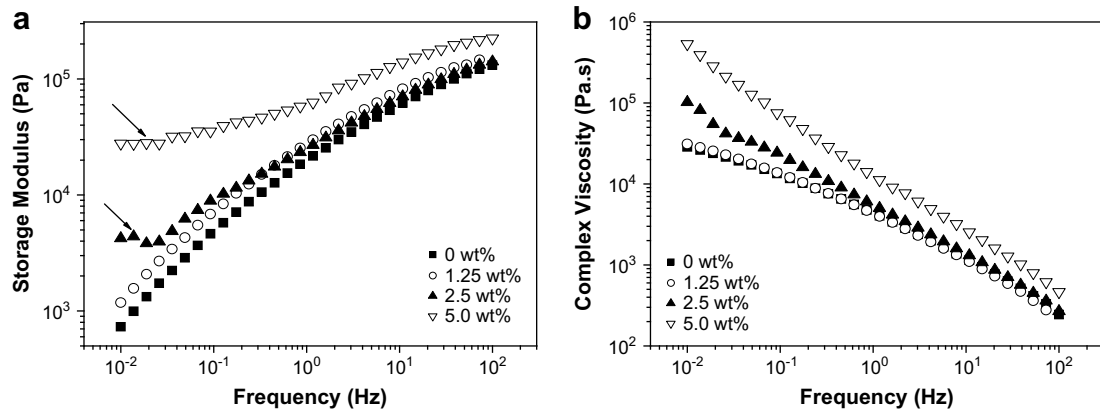


Fig. 8. Rheological properties of EVA melt containing different contents of f-MWCNTs: (a) storage modulus (G') and (b) complex viscosity (η^*).

the decrease of Van der Waals forces among f-MWCNTs. The interfacial bonding between PP and EVA is largely strengthened through the bridge effect of f-MWCNTs, which prevents the propagation of crack in the interface of PP and EVA, leading to the improvement of fracture toughness. On the other hand, it can be believed that the network structure of f-MWCNTs in cocontinuous PP/EVA (60/40) is more perfect than that in PP/EVA (80/20) with sea-island morphology. During the fracture process, the stress is easily to be transferred between matrix and EVA phase through the network structure of f-MWCNTs and the bridge between PP and EVA, inducing more homogeneous distribution of stress and avoiding the severe stress concentration which leads to the premature fracture of sample. Finally, one should notice that for PP/EVA (60/40) blend, there is a certain degree of interpenetration between the two phases, and the formation of the “dual-network structure” of f-MWCNTs and EVA in the blends possibly brings the similar effect on mechanical properties compared to the dynamic vulcanization in the thermoplastic elastomer blends [18].

Finally, it should be pointed out that in this work, the acid treatment of MWCNTs inevitably reduces the length of MWCNTs. As well known to all, the formation of the network structure is greatly dependent of the length of single CNT. The CNTs with larger length have more tendencies to span several ligaments of PP and EVA to show more apparent bridge effect on one side. On the other side, long CNTs are more favorable to the formation of network structure in both PP and EVA phase. Thus, the treatment of MWCNTs, which not only achieves the good dispersion but also maintains the large aspect ratio of CNTs, most likely results in more apparent in improving the fracture toughness of PP/EVA blends. Further work is being carried on to prove this hypothesis.

4. Conclusions

f-MWCNTs have been introduced into immiscible PP/EVA blends through the special melt-blending sequence. The measurement of the fracture toughness show that in the composites which exhibits the cocontinuous morphology, the addition of f-MWCNTs induces the great improvement of fracture toughness, and the fracture toughness increases with the increasing content of f-MWCNTs. However, in the composites which exhibit the typical sea-island morphology, f-MWCNTs have inconspicuous role in

improving the fracture toughness. Further results show that the continuous EVA phase is in favor of the network structure formation of f-MWCNTs. The great improvement of fracture toughness is ascribed to the bridge effect of f-MWCNTs in the interface and the formation of “dual-network structure” of f-MWCNTs and EVA. This work proves that the fracture toughness of immiscible polymer blends can be improved through the formation of a “dual-network structure” of filler and polymer.

Acknowledgements

The authors would like to express their sincere thanks to National Natural Science Foundation of China (50403019), Program for New Century Excellent Talents in University (NCET-08-0823) and Sichuan Youthful Science and Technology Foundation (07ZQ026-003) (PR China) for supporting this work. Authors greatly appreciated Prof. Qiang Fu (Sichuan University, China) for the illuminating discussion.

References

- [1] Gorga RL, Cohen RE. *J Polym Sci Part B Polym Phys* 2004;42(14):2690–702.
- [2] Zhao P, Wang K, Yang H, Zhang Q, Du RN, Fu Q. *Polymer* 2007;48(19):5688–95.
- [3] Dondero WE, Gorga RE. *J Polym Sci Part B Polym Phys* 2006;44(5):864–78.
- [4] Zhang XH, Zhang ZH, Xu WJ, Chen FC, Deng JR, Deng X. *J Appl Polym Sci* 2008;110(3):1351–7.
- [5] Zhang H, Zhang Z. *Eur Polym J* 2007;43(8):3197–207.
- [6] Ganß M, Satapathy BK, Thunga M, Weidisch R, Pötschke P, Jehnichen D. *Acta Mater* 2008;56(10):2247–61.
- [7] Ruan SL, Gao P, Yang XG, Yu TX. *Polymer* 2003;44(19):5643–54.
- [8] Khare RA, Bhattacharyya AR, Kulkarni AR, Saroop M, Biswas A. *J Polym Sci Part B Polym Phys* 2008;46(21):2286–95.
- [9] Li Y, Shimizu H. *Macromolecules* 2008;41(14):5339–44.
- [10] Maciel A, Salas V, Manero O. *Adv Polym Tech* 2005;24(4):241–52.
- [11] Pötschke P, Bhattacharyya AR, Janke A. *Polymer* 2003;44(26):8061–9.
- [12] Gao Y, Wang Y, Shi J, Bai HW, Song B. *Polym Test* 2008;27(2):179–88.
- [13] Blom HP, The JW, Rudin A. *J Appl Polym Sci* 1996;60(9):1405–17.
- [14] Yang JH, Zhang Y, Zhang YX. *Polymer* 2003;44(17):5047–52.
- [15] Sumita M, Sakata K, Hayakawa Y, Asai S, Miyasaka K, Tanemura M. *Colloid Polym Sci* 1992;270(2):134–9.
- [16] Yang H, Li B, Wang K, Sun TC, Wang X, Zhang Q, et al. *Eur Polym J* 2008;44(1):113–23.
- [17] Yang H, Zhang XQ, Qu C, Li B, Zhang LJ, Zhang Q, et al. *Polymer* 2007;48(3):860–9.
- [18] Kumar CR, Fuhrmann I, Karger-Kocsis J. *Polym Degrad Stab* 2002;76(1):137–44.